Local modes in $Al_{0.1}Cu_{0.9}$ and $(NH_4)_{0.1}K_{0.9}Cl$ in the coherent-potential approximation*

Theodore Kaplan and Mark Mostoller
Solid State Division, Oak Ridge National Laboratory, Oak Ridge, Tennessee 37830
(Received 13 July 1973)

Numerical techniques are described to apply the coherent-potential approximation (CPA) to mass defects in polyatomic cubic crystals, and to facilitate CPA calculations for light-mass defects in monatomic cubic crystals. Results are given for two alloys in which local modes have been observed by inelastic neutron scattering, $Al_{0.1}Cu_{0.9}$ and $(NH_4)_{0.1}K_{0.9}Cl$. The CPA is in good agreement with experiment for the local-mode peak position in the Al-Cu system, but the observed peak is much sharper. For the (NH_4-K)Cl alloy, the mass-defect CPA predicts a quasilocal resonant mode much lower in frequency than the experimental local-mode peak, showing the need to include force-constant changes in the theoretical model.

I. INTRODUCTION

When an isolated substitutional impurity is introduced into an otherwise perfect crystal, the host-lattice phonons can be scattered by the defect, and local or resonant modes may arise. A great deal of work has been done to elucidate the properties of lattice vibrations around isolated defects, so that rather elaborate calculations can now be compared with very detailed experimental results. To cite only one example, quite good agreement between calculation and experiment has been obtained for the infrared and Raman scattering of substitutional silver ions in sodium chloride.[1,2]

For substitutional alloys, multiple scattering, defect-defect interactions, possible clustering or ordering, and other effects make interpretation much more difficult, However, phonons often appear to remain as reasonably well-defined elementary excitations in alloys,[3-6] and broadened local modes split-off from the in-band modes have been observed at fairly high concentrations of light-mass impurities.[7-10] Inelastic neutron scattering is a particularly useful probe of phonons in alloys, since it can measure the frequencies and lifetimes of individual phonons, rather than sum or average properties like the density of states.

The simplest of the computationally tractable models for phonons in alloys is the virtual-crystal approximation, in which the force constants and masses for the alloy are taken to be concentration-weighted averages of those of the constituents. Although the phonon frequencies change continuously with concentration, phonons have infinite lifetimes in the virtual-crystal approximation, and no local or resonant modes are predicted.

In the average-scattering approach of Elliott and Taylor,[11] which is correct to lowest order in the concentration and includes certain terms of higher order, the in-band modes are both shifted and broadened, and local or resonant modes may occur. However, if a local mode is predicted above the host-lattice spectrum or in a gap, its lifetime is infinite in the Elliott and Taylor model.

The coherent-potential approximation (CPA), described by Taylor[12] for phonons and Soven[13] for electrons, is a mean-field theory in which the average scattering of phonons from any potential defect site in the effective crystal vanishes. The phonons are shifted and broadened in the in-band region in the CPA, and if a local mode splits off, it is broadened. For mass defects in monatomic cubic crystals, the CPA is relatively easy to implement. A complex self-energy must be determined self-consistently as a function of frequency from a quadratic equation in which one coefficient is the site-diagonal CPA Green's function; this Green's function can in turn be expressed as an integral of the product of the perfect-crystal density of states and an energy denominator containing the self-energy. The computational problems for monatomic cubic crystals are to find starting values for the self-energy, and to develop rapidly convergent procedures to track the self-energy as the frequency changes.

For mass defects in polyatomic cubic crystals (by which we mean cubic crystals having more than one kind of atom in the unit cell, like NaCl-type and zinc-blende materials), the CPA is much more difficult to apply, because the site-diagonal Green's function in the equation for the complex self-energy must be evaluated as an integral of a matrix product over the Brillouin zone, rather than as an integral of a scalar function over frequencies. Similar integrals over the Brillouin zone must be done to apply the CPA to mass defects in hcp and other more complicated crystals.

In this paper, we describe numerical techniques for the accurate application of the CPA to mass defects in polyatomic cubic crystals. Included is a straightforward application of the calculus of residues which solves the problem of finding starting values for the self-energy, and makes the CPA essentially automatic for monatomic cubic crystals. The requisite q-space integrations are done by summing over a regular mesh of boxes in the

Brillouin zone, with Monte Carlo sampling added in regions in which the integrand varies rapidly. Results at very low frequencies are obtained from the appropriate limiting expressions.

Section II briefly reviews the CPA for mass defects in cubic crystals and describes our computational procedures. In Sec. III, results are presented for two alloys in which local modes have been observed by inelastic neutron scattering, one a monatomic cubic metal (Al-Cu),[7] the other a diatomic cubic insulator [$(NH_4$-K)Cl].[8] Section IV draws some conclusions, and points to possible extensions.

II. THEORY AND COMPUTATIONS

The basic equations of the CPA for mass defects have been given by Taylor.[12] For monatomic cubic crystals, the CPA phonon Green's function, $\underline{G}^0(\vec{q},\omega)$, satisfies the equation

$$\underline{I} = \{M\omega^2[1-\epsilon(\omega)]\underline{I} - \underline{\Phi}(\vec{q})\}\cdot \underline{G}^0(\vec{q},\omega)\ , \tag{1}$$

where $\underline{I}$ is the unit matrix, M is the atomic mass of the host atoms, ω is the frequency, and $\underline{\Phi}(\vec{q})$ is the force constant matrix for the perfect crystal at the wave vector $\vec{q}$. The dimensionless self-energy $\epsilon(\omega)$ must be determined self-consistently from

$$0 = \epsilon(\omega) - c\theta + \epsilon(\omega)[\epsilon(\omega)-\theta]\,G_0(\omega)\omega^2\ . \tag{2}$$

Here, $\theta = (M - M_d)/M$, where M_d is the defect mass, c is the concentration, and $G_0(\omega) = MG^0_{xx}(l,l;\omega)$ is the site-diagonal Green's function, which is independent of the site l, and can be expressed as an integral over the perfect-crystal density of states $\nu(\omega)$,

$$G_0(\omega) = \int d\omega' \frac{\nu(\omega')}{\omega^2[1-\epsilon(\omega)]-\omega'^2}\ . \tag{3}$$

For polyatomic cubic crystals with defects at the side β in the unit cell, the CPA Green's function is the solution of the equation

$$\underline{I}\,\delta_{b,b'} = \sum_{b''}\{M_b\omega^2[1-\epsilon(\omega)\,\delta_{b,\beta}]\underline{I}\,\delta_{b,b''} - \underline{\Phi}(b,b'';\vec{q})\}\cdot \underline{G}^0(b'',b';\vec{q},\omega)\ , \tag{4}$$

where M_b is the host mass of the atom at the site b in the unit cell. The complex self-energy $\epsilon(\omega)$ must again be found self-consistently from equation (2). Now, however, the site-diagonal Green's function in Eq. (2) is $G_0(\omega) = M_\beta G^0_{xx}(l\beta, l\beta;\omega)$, which cannot be expressed as an integral over frequencies. Instead, it must be evaluated as an integral

$$G_0(\omega) = \tfrac{1}{3}\mathrm{Tr}\int_{BZ}\frac{d^3q}{8\pi^3}\{\underline{I} - \epsilon(\omega)\omega^2[M_\beta\underline{P}(\beta,\beta;\vec{q},\omega)]\}^{-1} \cdot [M_\beta\underline{P}(\beta,\beta;\vec{q},\omega)]\ . \tag{5}$$

In terms of the polarization vectors $\vec{\sigma}(\vec{q},\beta,j)$ and frequencies $\omega_j(\vec{q})$ for the various branches of the phonon spectrum, the perfect-crystal Green's function $\underline{P}(\beta,\beta;\vec{q},\omega)$ is given by

$$M_\beta\underline{P}(\beta,\beta;\vec{q},\omega) = \sum_j \frac{\vec{\sigma}^*(\vec{q},\beta,j)\,\vec{\sigma}(\vec{q},\beta,j)}{\omega^2-\omega_j^2(\vec{q})}\ . \tag{6}$$

One problem encountered in applying the CPA is to find a starting value for the self-energy at some particular frequency, or if local modes split off, to find starting values in both the in-band and local mode regions. To solve this problem, we use a theorem of the complex integral calculus.[14] If $f(z)$ is a meromorphic function inside a closed contour C, and is not zero at any point on C, then

$$\frac{1}{2\pi i}\int_C \frac{f'(z)}{f(z)}\,dz = n_0 - n_p\ , \tag{7}$$

where n_0 is the number of zeros and n_p the number of poles of $f(z)$ inside C, and a pole or zero of order m must be counted m times. If the integrand is multiplied by z, then

$$\frac{1}{2\pi i}\int_C \frac{zf'(z)}{f(z)}dz = \sum z_0 - \sum z_p \tag{8}$$

gives the difference between the sums of the values of the zeros and poles, where again a pole or zero of order m must be repeated m times. Similar expressions hold for higher powers of z.

From Eq. (2), we define the function

$$f(\epsilon) = \epsilon - c\theta + \epsilon(\epsilon-\theta)\,G_0(\omega;\epsilon)\,\omega^2\ , \tag{9}$$

which has zeros but no poles off the real ϵ axis since $G_0(\omega;\epsilon)$ as determined from Eq. (3) or (5) is regular for $\mathrm{Im}\,\epsilon \neq 0$. Performing the integration (7) numerically over a closed contour in the upper half ϵ plane tells us whether there are any roots within the contour; if there is one, the integral (8) gives its value.

Once starting values have been obtained for $\epsilon(\omega)$, a local method is employed to track the self-energy as a function of frequency. Specifically, we use a rapidly convergent modification of the Newton-Raphson technique. If this method loses the self-energy, then recourse is taken again to the contour integral procedure. This combination of contour integration and local tracking makes CPA calculations for mass defects in monatomic cubic crystals virtually automatic, and greatly facilitates the calculations for polyatomic materials, where even if no local-mode band splits off, it is not convenient to start at low frequencies and work upward.

A two-step procedure is also used to evaluate the integral over the Brillouin zone in Eq. (5) for the site-diagonal Green's function for polyatomic crystals. The irreducible $\frac{1}{48}$th of the zone is first broken up into a large number of small boxes, as in the Gilat-Raubenheimer method[15] for calculating

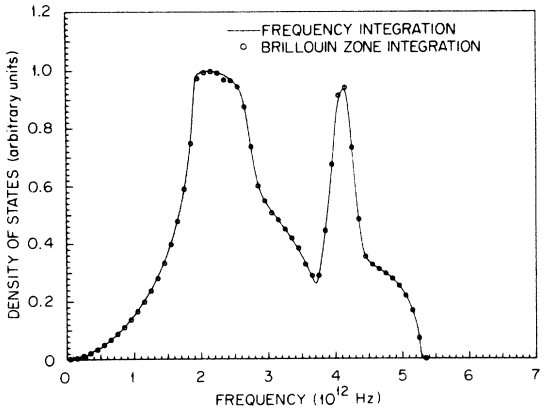

FIG. 1. CPA density of states for $Ag_{0.1}Au_{0.9}$, as obtained self-consistently by frequency integration from Eqs. (2) and (3), and by integration over the Brillouin zone from Eqs. (2) and (5).

perfect crystal densities of states. In most of these boxes, the integrand in Eq. (5) is slowly varying, and the contributions to $G_0(\omega)$ are to a a good approximation given by the products of the value at the center of the box and its volume, weighted appropriately if part of the box extends outside the irreducible $\frac{1}{48}$th. If the imaginary part of $\epsilon(\omega)$ is small, however, the integrand will vary rapidly in regions of q space where the CPA phonons have frequencies close to ω. In these regions, Monte Carlo sampling is done. This procedure works well in reasonable amounts of computer time except at low frequencies, but here, Taylor-series expansions for the various quantities of the CPA can be employed. For example, $\mathrm{Re}\epsilon(\omega)$ approaches $c\theta$ as an even power series in ω, while $\mathrm{Im}\epsilon(\omega)$ is an odd function which begins at third order in the frequency.

To test the accuracy of our integration procedure, we did a CPA calculation for a 10% silver-gold alloy ($Ag_{0.1}Au_{0.9}$), evaluating $G_0(\omega)$ first by intergrating over frequencies as called for in Eq. (2), and then by performing the equivalent integration over the Brillouin zone of Eq. (5) for this monatomic cubic alloy. The irreducible $\frac{1}{48}$th of the zone was broken up into 770 boxes for the q-space integration. Figure 1 shows a comparison of the results of the two methods for the density of states. The agreement is excellent, and within the convergence criteria used in the iterative calculation of $\epsilon(\omega)$. The great difference, of course, is in the amount of computer time required for the two calculations; it took roughly half a minute of IBM 360-91 time to generate the smooth curve in Fig. 1 by ω integration, and about 20 min to determine the circled points by integration over the Brillouin zone, or an average of roughly 20 sec per point.[16]

III. RESULTS

Local modes may arise around impurities if the defect mass is lighter than that of the host, or if the force constants between the defect and its neighbors are much stiffer than those connecting host-lattice ions, or through a combination of these two causes. Two alloys in which local modes have been observed by inelastic neutron scattering at modest concentrations of light-mass impurities are Al-Cu[7] and $(NH_4$-K)Cl.[8] In this section we will present the results of CPA mass-defect calculations for these two alloys, each for a 10% concentration of the light-mass constituent, and show how well these results agree with experiment.

For the $Al_{0.1}Cu_{0.9}$ system, a virtual crystal model was used for the force constants, that is, the force constants for the "perfect crystal" were taken to be $\underline{\Phi} = 0.1\underline{\Phi}_{Al} + 0.9\underline{\Phi}_{Cu}$. This shifts the phonon frequencies down by a small amount, since the first-neighbor force constants for aluminum[17] are smaller than those for copper.[18]

Figure 2 compares the CPA density of states

$$\nu'(\omega) = -(2\omega/\pi)\,\mathrm{Im}\,[M(1-\epsilon(\omega))\,G^0_{xx}(l,l;\omega)]\,, \quad (10)$$

with the "perfect-crystal" result, which was obtained by the Gilat-Raubenheimer method. The effect of alloying in the CPA is to smooth out the in-band modes and shift the band edge down, and to produce a broad local-mode band centered at about 8.9×10^{12} Hz. The real and imaginary parts of the self-energy are shown in Fig. 3. Since $\mathrm{Im}\epsilon(\omega)$ is small except in the local-mode region, only the local modes are expected to be significantly broadened by the disorder.

Figure 4 is a comparison of the calculated results with experimental data of Nicklow *et al.*[7] for the inelastic neutron scattering at the zone bound-

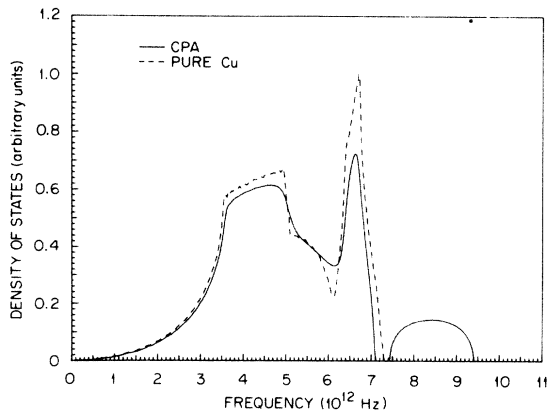

FIG. 2. CPA density of states for $Al_{0.1}Cu_{0.9}$ compared to the "perfect-crystal" density of states of pure Cu but with virtual crystal-force constants.

ary point $\vec{q} = (\frac{1}{2}, \frac{1}{2}, \frac{1}{2})(2\pi/a)$. To obtain the calculated curve, we summed the coherent and incoherent contributions,[11,12,19,20] and then folded in a Gaussian to incorporate the experimental resolution. The rapid rise in the experimental values below the LA in-band peak is due to high-order diffraction processes in the monochromator and analyzer.

The agreement between the CPA and experiment for the local-mode peak position is surprisingly good. The outer electronic configurations of aluminum and copper are quite different, so one might expect force constant changes to play a larger role than Fig. 4 seems to indicate. However, the CPA does a rather poor job in fitting the sharpness and intensity of the local mode relative to the in-band peak; this is understated in Fig. 4, since the observed phonon peaks are riding on the downslope of a lower frequency peak arising from another scattering process. The experimental results also contain an interesting but barely resolved hint of structure at about 9.2×10^{12} Hz in the local mode region. Such structure, if confirmed, would reflect correlations which lie beyond the scope of a single-site CPA. Pair and higher correlation effects are expected even for purely random alloys,

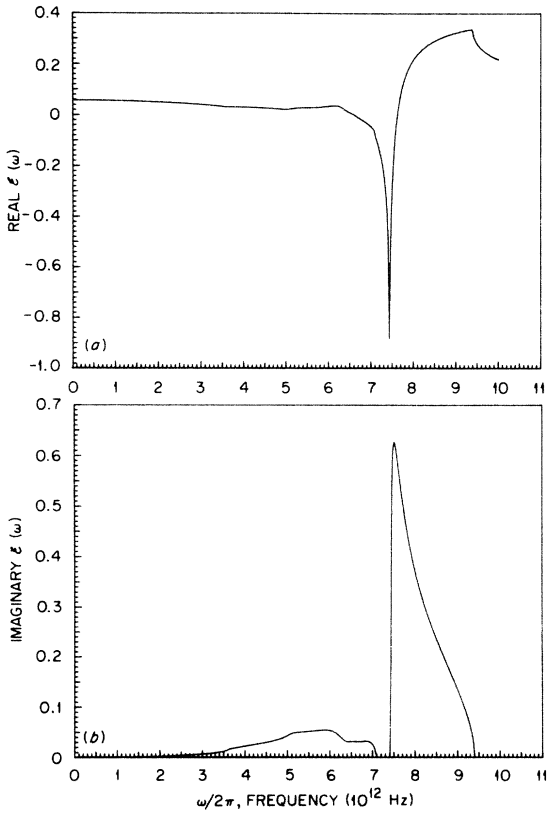

FIG. 3. Complex self-energy $\epsilon(\omega)$ for $Al_{0.1}Cu_{0.9}$.

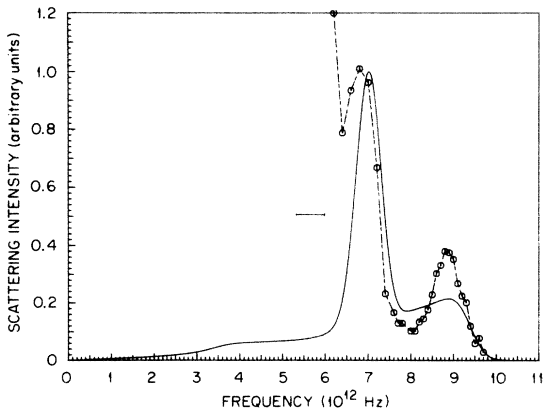

FIG. 4. Calculated and observed inelastic neutron scattering from $Al_{0.1}Cu_{0.9}$ for the scattering wave vector $\vec{Q} = (\frac{1}{2}, \frac{1}{2}, \frac{1}{2})(2\pi/a)$. The experimental points are from Nicklow *et al.* (Ref. 7) with background subtracted, and the horizontal bar shows the experimental resolution.

and may be enhanced by clustering or ordering. In this connection, Borie and Sparks[21] have observed short-range ordering of the aluminum atoms in $Al_{0.16}Cu_{0.84}$ alloys.

The disagreement between the CPA and experiment for the position of the in-band LA mode in Fig. 4 is typical for this alloy; the in-band phonon frequencies predicted by the mass-defect CPA, like those found from low-concentration limit expressions, lie generally above the observed peaks. As suggested by Nicklow *el al.*, this may result at least in part from the expansion of the lattice which occurs when the aluminum is added to the copper. The attendant general lowering of the in-band phonon frequencies could be modeled by further decreasing the force constants of the "perfect crystal" used in the CPA calculations. However, calculations that we have done show that lowering the in-band modes in this way also has the undesirable effect of lowering the local-mode peak. The change in volume on alloying and the difficulties encountered in matching both the in-band and local-mode frequencies are indications that the forces do vary significantly around the different constituents.

The work of Smith *el al.*[8] focussed on the local and torsional modes of small concentrations of ammonium ions in KCl. Although the NH_4^- ion is roughly the same size as the potassium ion, they found that isolated mass defect theory predicted a resonant mode near the top of the perfect-crystal spectrum, and that a nearest-neighbor force constant increase of the order of 25% was necessary to move the impurity mode to its observed position above the band. Not surprisingly, the mass-defect CPA calculations for the 10% alloy

also predict a resonant mode near the top of the perfect-crystal spectrum, which illustrates the necessity of finding some way to incorporate force-constant changes for phonons in alloys.

Figure 5 shows the complex self energy for $(NH_4)_{0.1}K_{0.9}Cl$, and Fig. 6 compares the CPA density of states for the alloy,

$$\nu'(\omega) = -(\omega/\pi)\,\mathrm{Im}\sum_b M_b(1-\epsilon(\omega)\,\delta_{b,\beta})\,G^0_{xx}(lb, lb; \omega) \tag{11}$$

to that of pure KCl, as determined by the Gilat-Raubenheimer method from the shell model used for the perfect crystal. The small hump at about 5.75×10^{12} Hz in the alloy density of states is the quasilocal resonant mode. Otherwise, the CPA curve differs very little from that for pure KCl, primarily because only 5% of the total number of atoms in the crystal change when 10% of the positive ions are replaced by impurities. The irreducible $\frac{1}{48}$th of the Brillouin zone was broken up into 770 boxes for the CPA calculations, which for all of the results given for this material took something of the order of 30 min of IBM 360-91 time, or roughly 25 sec per frequency point on the average.

Figure 7 compares the calculated and observed neutron scattering for the scattering wave vector

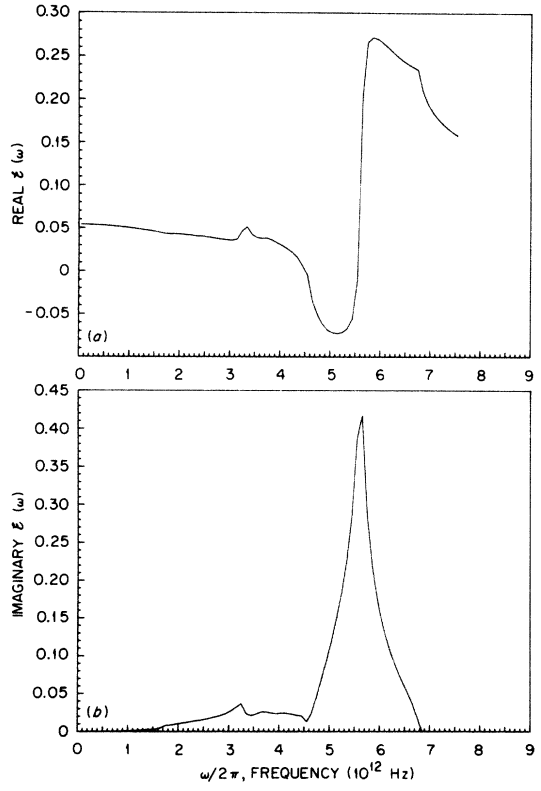

FIG. 5. Complex self-energy $\epsilon(\omega)$ for $(NH_4)_{0.1}K_{0.9}Cl$.

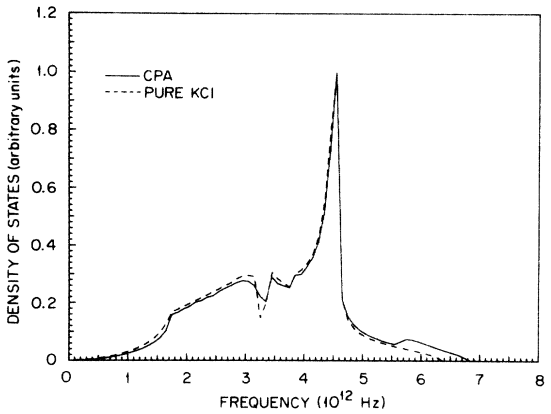

FIG. 6. CPA density of states for $(NH_4)_{0.1}K_{0.9}Cl$ compared to that for pure KCl.

$\vec{Q} = (2.7, 2.7, 3.3)(2\pi/a)$. The calculated in-band TO peak at 4.05×10^{12} Hz falls slightly below the observed peak. However, the calculated quasilocal mode, which is the major peak at 5.85×10^{12} Hz, is far below the experimental local mode peak above 7×10^{12} Hz. The experimental points in Fig. 7 are unpublished data from experiments on a 10% single crystal,[22] with much more scatter in the local-mode region than in the published work, which was done on substantially larger polycrystalline and powder samples.[8] In the measurements done on the 10% single crystal, it has proven difficult to obtain good data spanning a frequency range from below an in-band to above the local mode. For several scattering vectors for which the statistics were better, there were in-band peaks near the frequency of the CPA resonant

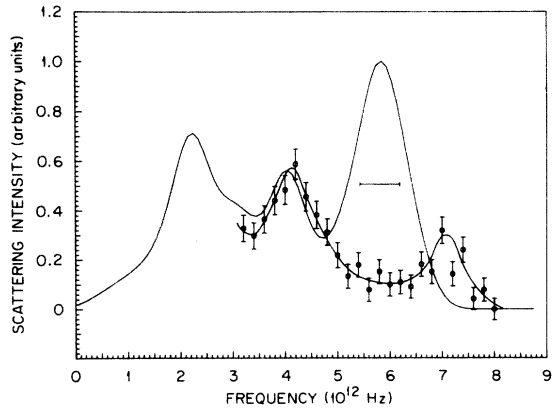

FIG. 7. Calculated and observed inelastic neutron scattering from $(NH_4)_{0.1}K_{0.9}Cl$ for the scattering wave vector $\vec{Q} = (2.7, 2.7, 3.3)(2\pi/a)$. The horizontal bar shows the experimental resolution, and background has been subtracted from the experimental data.

mode, so that a comparison of calculation and experiment for these scattering vectors would be misleading.

The calculated curve in Fig. 7 is the sum of the coherent and incoherent scattering,[23] convolved with a Gaussian resolution function. The major uncertainty in the calculated results is the large incoherent scattering cross section of the hydrogens of the ammonium ion, which varies strongly with environment and neutron energy. In the absence of direct measurement of this cross section for the $(NH_4\text{-}K)Cl$ system, a value of 50 b was chosen as a reasonable figure from the work of Rush, Taylor, and Havens[24] on various ammonium halides. As shown in Fig. 8, the incoherent scattering is responsible for virtually all of the local-mode peak, and provides a background on which the coherent in-band peaks ride.

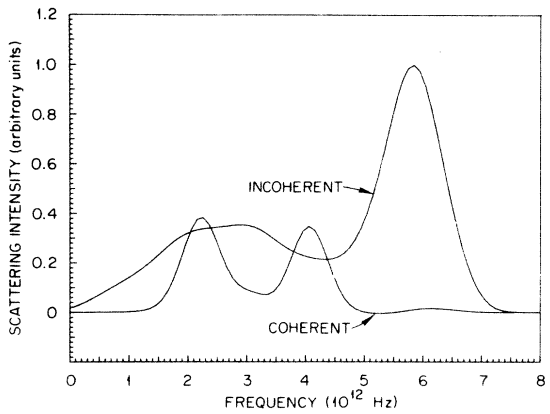

FIG. 8. Coherent and incoherent contributions to the calculated scattering cross section of $(NH_4)_{0.1}K_{0.9}Cl$ for the scattering wave vector $\vec{Q} = (2.7, 2.7, 3.3)(2\pi/a)$.

IV. CONCLUSION

We have described numerical methods to apply the CPA to mass defects in polyatomic cubic crystals, and to automate the CPA for monatomic cubic crystals. Essentially the same procedures can be followed for the hcp and other lattices, although noncubic systems are more complicated in that the complex self-energy has more than one independent component.

The comparison of CPA mass-defect calculations with experimental results for $(NH_4\text{-}K)Cl$ indicates the need to incorporate force-constant changes in the theoretical model. In a subsequent paper, we will describe one way in which the CPA can be extended to include force-constant changes. For Al-Cu, the neutron-scattering data also suggests that practical ways must be found to treat pair and higher correlation effects. However, the amounts of time required to do CPA mass-defect calculations in polyatomic cubic crystals indicate that future refinements in theory may not be easy to apply.

ACKNOWLEDGMENTS

We are grateful to Dr. J. A. Rome for providing the programs to do the contour integrals which locate roots of the self-energy equation. We are also indebted to Dr. H. G. Smith, Dr. R. M. Nicklow, Dr. N. Wakabayashi, and Dr. M. Neilsen for furnishing experimental data and interpretation, and to Dr. W. H. Butler and Dr. J. S. Faulkner for helpful discussions.

*Research sponsored by the U. S. Atomic Energy Commission under contract with Union Carbide Corp.

[1]G. P. Montgomery, Jr., Miles V. Klein, B. N. Ganguly, and R. F. Wood, Phys. Rev. B 6, 4047 (1972).

[2]Mark Mostoller and R. F. Wood, Phys. Rev. B 7, 3953 (1973).

[3]E. C. Svensson and W. A. Kamitakahara, Can. J. Phys. 49, 2291 (1971).

[4]W. A. Kamitakahara and B. N. Brockhouse, in *Neutron Inelastic Scattering* 1972 (IAEA, Vienna, 1972), p. 73.

[5]H. G. Smith and W. Gläser, in *Phonons*, edited by M. Nusimovici (Flammarion, Paris, 1971), p. 145.

[6]W. J. L. Buyers and R. A. Cowley, in *Neutron Inelastic Scattering* (IAEA, Vienna, 1968), Vol. I. p. 43.

[7]R. M. Nicklow, P. R. Vijayaraghavan, H. G. Smith, G. Dolling, and M. K. Wilkinson, in Ref. 6, p. 47.

[8]H. G. Smith, N. Wakabayashi, and R. M. Nicklow, in Ref. 4, p. 103.

[9]N. Wakabayashi, R. M. Nicklow, and H. G. Smith, Phys. Rev. B 4, 2558 (1971).

[10]B. Mozer, in Ref. 6, p. 55.

[11]R. J. Elliott and D. W. Taylor, Proc. R. Soc. A 296, 161 (1967).

[12]D. W. Taylor, Phys. Rev. 156, 1017 (1967).

[13]P. Soven, Phys. Rev. 156, 809 (1967).

[14]E. T. Copson, *An Introduction to the Theory of Functions of a Complex Variable* (Oxford U. P., London, 1960), p. 118.

[15]G. Gilat and L. J. Raubenheimer, Phys. Rev. 144, 390 (1966).

[16]D. W. Taylor [Solid State Commun. 13, 117 (1973)] has done some CPA calculations for mixed alkali-halide crystals by adding a finite imaginary part to the energy denominators of the perfect-crystal Green's functions in the integral (5), and summing over a smaller mesh of points (~ 170) in the irreducible $\frac{1}{48}$th of the Brillouin zone than we employ. This procedure has the advantage of speed, and is useful in identifying trends and major features predicted by the CPA. However, in calculations we have done using this method, we have found that it is necessary to optimize the finite imaginary part added to the energy denominators in order to avoid oversmoothing or the introduction of extraneous structure. Furthermore, band trailing and some distortion of the spectrum persist even for the optimum choice.

[17]Leon Van Hove, Phys. Rev. 95, 249 (1954).

[18]G. Gilat and R. M. Nicklow, Phys. Rev. 143, 487 (1966).

[19]R. M. Nicklow, G. Gilat, L. J. Raubenheimer, and M. K. Wilkinson, Phys. Rev. 164, 922 (1967).
[20]W. A. Kamitakahara and D. W. Taylor (unpublished).
[21]B. Borie and C. J. Sparks, Jr., Acta Crystallogr. 17, 827 (1964).
[22]H. G. Smith, N. Wakabayashi, and R. M. Nicklow (private communication).
[23]For the calculation of the neutron-scattering cross section, the ammonium ion was treated as a rigid tetrahedron which could randomly assume its two distinct orientations, with an N-H separation of 1.04 Å. The formulas for the incoherent and coherent scattering cross sections in the CPA for the sodium-chloride structure are straightforward extensions of those for Bravais lattices discussed in Refs. 11, 12, 17, and 18.
[24]J. J. Rush, T. I. Taylor, and W. W. Havens, Jr., Phys. Rev. Lett. 5, 11 (1960).